Prepublished copy

Nature Environment & Pollution Technology

This is a peer-reviewed prepublished version of the paper

Original Research

Optimization of HHO Gas Production in Alkaline Dry-Type HHO Kit Using Various Electrode and Electrolyte Configurations

M.B.D.K. Siriwardena[1], A.R. Nihmiya[2†], Udara S.P.R. Arachchige[3] and Gamunu S. Arachchige[4]

[1,2] Department of Civil & Environmental Technology,
Faculty of Technology, University of Sri Jayewardenepura, Sri Lanka; mbdksiriwardena@gmail.com[1], nihmiya@sjp.ac.lk[2]
[3] Department of Chemical & Petroleum Engineering, University of Calgary, Canada; udara.pahalagamarana@ucalgary.ca[3]
[4] Department of Process, Energy and Environmental Technology, Faculty of Technology, Natural Sciences and Maritime Sciences, University of South-Eastern Norway, Norway; gamunu.samarakoon@usn.no[4]
† Corresponding author: A.R. Nihmiya; nihmiya@sjp.ac.lk
ORCID IDs of Authors 0009-0005-5331-6417[1], 0000-0003-0903-8753[2] ,0000-0001-8602-5257[3]

Abstract: This research investigates the optimization of a dry-type alkaline HHO kit for efficient oxyhydrogen (HHO) gas production, targeting applications in small (two-wheel vehicle) internal combustion engines (ICE). Key experimental parameters were evaluated to enhance gas production and system efficiency, including voltage, electrode configuration, electrolyte type, and concentration. Sodium hydroxide (NaOH) was identified as a more effective electrolyte than potassium hydroxide (KOH) due to its lower electronegativity, which contributes to accelerating HHO gas production. The highest overall efficiency, 24.6%, was achieved with a 0.1M NaOH solution using stainless steel (SS) as the anode and Titanium (Ti) as the cathode, and SS paired with graphite scored 23.1%. Voltage levels positively influenced gas production, although higher potential resulted in electrode surface oxidation and decreased efficiency. The optimum voltage range of 4.5V to 5.2V for SS with graphite and 4.2V to 5.2V for SS with Ti configurations were provided. The study concludes that the SS-Ti and SS-Graphite configurations are optimal options for HHO gas production, minimizing heat generation and energy consumption while enhancing gas output. These findings suggest significant potential for improving fuel efficiency and reducing greenhouse gas emissions in two-wheel vehicle four-stroke gasoline engines (100cc to 150cc).

Key Words	Alkaline Electrolyser, Dry-type Generator, Electrolysis, Green Energy, Internal Combustion Engine, Oxyhydrogen Gas, Oxyhydrogen Generator
DOI	https://doi.org/10.46488/NEPT.2025.v24i03.D1728 (DOI will be active only after the final publication of the paper)
Citation of the Paper	M.B.D.K. Siriwardena, A.R. Nihmiya, Udara S.P.R. Arachchige and Gamunu S. Arachchige, 2025. Optimization of HHO Gas Production in Alkaline Dry-Type HHO Kit Using Various Electrode and Electrolyte Configurations. *Nature Environment and Pollution Technology*, 24(3), D1728. https://doi.org/10.46488/NEPT.2025.v24i03.D1728

1. INTRODUCTION

The trend of renewable energy resource utilization has increased with higher demand, driven by increasing awareness of the harmful effects of fossil fuel consumption. It has been identified as a significant contributor to greenhouse gas (GHG) emissions, leading to climate change and global warming in transportation. The growing

concern over fossil fuel depletion of non-renewable energy sources has further highlighted the urgent need to transition to green energy sources, such as solar, wind, and hydropower (Jones, 2014). These have appeared viable and cleaner energy options over general fossil fuel-consumed internal combustion engines (ICE). It has been blown up by the global focus on emission reductions and meeting international climate milestones (Zohuri Bahman, 2018; Chinguwa, Jen, and Akinlabi, 2020).

Furthermore, hydrogen (H_2) plays a vital role in the evolution of alternative fuels because of its purity and higher energy content compared with others. Hence, it can be supported to achieve the circular economy through sustainable development goals (SDGs), affordable and clean energy (SDG 7), industry innovation (SDG 9), and climate action (SDG 13) (Rinawati *et al.*, 2022). H_2 can lower GHG emissions, aligning with global efforts to address climate change (Khandal *et al.*, 2022). H_2 offers a unique advantage in providing a closed-loop energy system, utilizing renewable resources to meet energy demands in a cleaner, more efficient manner (Mesut Yurukcu *et al.*, 2021).

Different technologies can be applied to produce H_2, such as Steam Methane Reforming (SMR), Partial Oxidation, Coal Gasification, and Electrolysis (Bard A. J., 2001; Zohuri Bahman, 2018). The electrolysis process by water splitting is better aligned with the ICE application, most commonly due to its purity and applicability (Slobodan Petrovic and Eklas Hossain, 2020). Direct current (DC) electricity is required as the power source to generate HHO gas (Newman, 2012). Hence, this method is named green H2 gas (Bard A. J., 2001). HHO generators comprise an electrolyte consisting of two electrodes, the anode and cathode, configured as a sandwich, and electrolytes enter inside that chamber fixed with a gasket. As mentioned, the type of specific electrolyte solution used in HHO generators may differ from the purpose of the application (Huang and Wang, 2020; F. Wang, 2022). During electrolysis, an electric current is taken through the electrolyte solution, leading to the decomposition of water molecules into H_2 and Oxygen (O_2), and the whole process of HHO generation is represented in the following 1, 2, and 3 Equations from (Bard A. J., 2001; Fuller and Harb, 2018).

$$2H_2O_{(l)} + Energy_{(electricity)} \rightarrow 2H_{2(g)} + O_{2(g)} \quad (1)$$

Half-cell chemical reaction of Anode (Oxidation)

$$2H_2O_{(l)} \rightarrow O_{2(g)} + 4H^+_{(aq)} + 4e^- \quad (2)$$

Half-cell chemical reaction of Cathode (Reduction)

$$2H_2O_{(l)} + 2e\text{-} \rightarrow H_{2(g)} + 2OH^-_{(aq)} \quad (3)$$

In the electrolysis process, there are two main types of alkaline generators separated by considering cell configuration, such as Wet-type and dry-type HHO generators in Fig. 1. Alkaline-wet HHO generators mainly use electrolytes of sodium hydroxide (NaOH) or potassium hydroxide (KOH) in a liquid state. The electrode stack sink is filled with electrolyte solutions in the container. Dry-type HHO generators only touch electrolytes inside the gasket with the electrode as a sandwich, which is used to fix wells except for leakages (Wilberforce and Olabi, 2020). They operate with a dry cell configuration with liquid electrolyte. For instance, dry-type HHO generators are preferred due to their efficiency. Unlike wet cells, they do not submerge electrodes in liquid but instead use conductive material to facilitate the reaction (Sivakumar *et al.*, 2021).

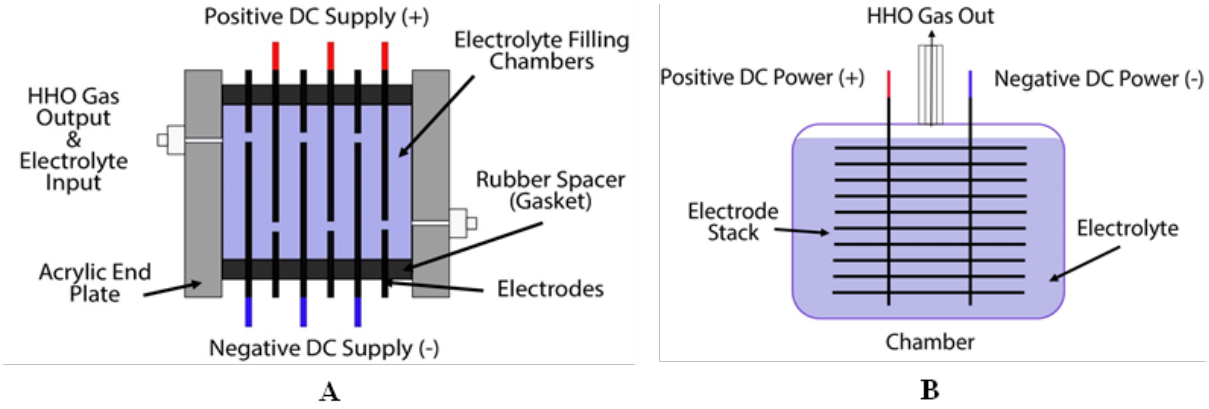

Fig. 1: Dry-Type Alkaline Electrolyser (A), Wet-Type Alkaline Electrolyser (B)

While HHO gas can be integrated with internal combustion engines (ICEs), it has been explored as a fuel additive to enhance ICE performance and improve the purity of transportation emissions. Studies by (Arjun T. B. et al., 2019a; Chinguwa, Jen, and Akinlabi, 2020) reported that integrating HHO gas into gasoline engines improves combustion efficiency and minimizing harmful emissions of GHGs due to the improved engine performance of brake power by reducing fuel consumption. Specifically, (Chinguwa, Jen, and Akinlabi, 2020) demonstrated a 10% increase in thermal efficiency and a 34% reduction in fuel consumption when HHO gas was blended with gasoline in a 0.1M NaOH electrolyte solution by following alkaline electrolysis. Integrating HHO gas into ICEs also addresses common challenges like detonation and flashback. Blending HHO gas with gasoline at a suitable ratio (1:8) to prevent engine knock, detonation, pre-ignition, and flashback could reduce CO and HC emissions by 26% and 27%, and SAC levels decreased to 9%, respectively (Arjun T. B. *et al.*, 2019a). This improvement is attributed to the higher energy density of H_2, which promotes a more complete combustion process.

Nevertheless, several challenges remain in optimizing the HHO system with ICEs. Typically, electrode degradation due to oxidation is a critical issue, as it affects the long-term durability and efficiency of the system. Studies by (Bockris, Gamboa-Aldeco, and Reddy, 2002; Fuller and Harb, 2018) explored the impact of electrode material choices on system performance, emphasizing the need for corrosion-resistant materials such as titanium (Ti) and stainless steel (SS). A significant challenge is heat and vapor production during electrolysis. Hence, it requires improvements in critical areas to enhance the efficiency of HHO production by electrode materials and electrolyte solutions (Arjun T. B. *et al.*, 2019b; Rusdianasari, Yohandri Bow and Tresna Dewi, 2019).

Additionally, (Khandal *et al.*, 2022) highlighted that maintaining an optimal electrolyte concentration is crucial to minimizing energy losses and heat generation. Hence, recent innovations are being conducted to improve combining electrode materials to leverage their complementary properties. For instance, (Rimkus, Mejeras, and Matijošius, 2023) found that combining SS with graphite resulted in a higher gas production rate than single-material configurations.

This study aims to improve the design of the alkaline dry-type HHO kit and its efficiency by examining the effects of various electrode materials, electrolyte types, and their concentrations on HHO gas production. This research seeks to enhance the performance of the HHO kit system integrated with selected ICEs by minimizing heat and vapor generation during electrolysis. It facilitates the prevention of engine failures by identifying significant issues and contributes to a more sustainable and environmentally friendly transportation sector.

2. MATERIALS AND METHODS

2.1. Regents and materials

SS sheets, Graphite sheets, and Ti sheets were purchased from AliExpress retail service by Alibaba.com in China. EPDM rubber sheet and copper sheet were used. The chemicals NaOH and KOH, as well as distilled water, were used with more than 99.98% purity. Plexiglass (Acrylic) sheet and tube (transparent), polyvinyl-chloride (PVC) endcap, pneumatic fittings, and hose were used. YAXUN 1502DD^{+} bench power supply (12V/2A DC), UNI-T UT136^{+} digital multimeter (potentiometer), Peristaltic DC pump, and AFM0725H00 gas flow meter were utilized. The solvent cement of S-Lon 10min rapid was used.

2.2. Design and Construction of the HHO Generator

The developed HHO kit consisted of two central units: the generator unit and the separator/bubbler unit. Table 1 presents the specifications of the developed Alkaline Dry-Type HHO kit.

Table 1: Specifications of Developed Alkaline Dry-Type HHO Kit Parameters

Parameter	Unit	Specification
Operating Voltage (DC.)	*V*	1.4 – 7.0
Working Current range	*mA*	1 – 700
Max Cell Power	*W*	4.9
The volume of the HHO generator	cm^3	1.6
Reactive area of electrodes	cm^2	4
Solution Molarity	$Moles/cm^3$	0.08 – 0.12
The volume of the gas separator	cm^3	157

The generator unit was built using a single cell, which included one anode and one cathode. The electrode plates were arranged in layers and separated by gaskets made from EPDM rubber. The EPDM rubber is known for its resistance to high temperatures and helps prevent leaks. Electrode plates and gaskets were rigidly connected to copper terminals, which were used to supply power. The frame plate of the generator was made from transparent plexiglass, and it had eight holes drilled to connect the electrolyte pipes and gas outlets. The generator unit was assembled using SS nuts and bolts, ensuring a tight and secure fit. The gas outlet's hole size was 4M, and the others were 2 M. The bubbler unit was constructed from PVC end caps and a transparent acrylic tube. The Bubbler unit was fixed with an acrylic tube and PVC endcaps. It was bonded by solvent cement to make seals to prevent electrolyte leakages. Fig. 2 illustrates the design followed to construct the kit, and Table 2 illustrates measures of all materials used for the HHO kit.

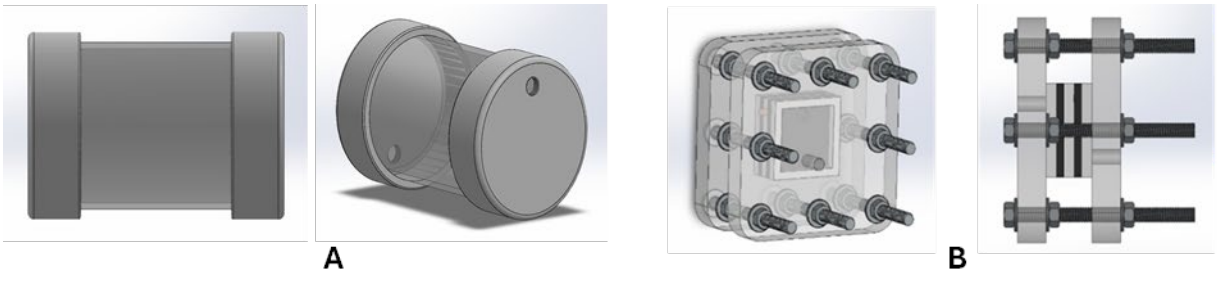

Fig. 2: Design of Bubbler Unit (A), Design of Generator Unit (B)

Table 2: Materials and Equipment for HHO Kit and Associated Components

Component/Application	Materials and Equipment	Dimensions/Quantity
HHO Generator Unit	Plexiglass (Acrylic) 8mm thick	80cm^2

	SS grade 306 sheet	$25mm \times 25mm$
	Graphite sheet 2mm thick	$25mm \times 25mm$
	Ti grade II sheet	$25mm \times 25mm$
	EPDM rubber sheet 3mm thick	$25mm \times 25mm$
	copper sheet 1mm thick	$4mm \times 2mm$
Bubbler Unit	Polyvinyl-chloride (PVC) endcap	Φ 50mm
	Plexiglass (Acrylic) tube	Φ 50mm
Chemicals and Solvents	NaOH and KOH	$6.2g + 4.8g$
	Distilled water	120ml
Fitting and Fixings	Pneumatic fittings	$6M$
	Pneumatic hose	Φ 4mm
	SS nuts and bolts	4M
Bonding Glue	S-Lon solvent cement	5ml
Testing Equipment	Bench power supply	12V/2A
	Potentiometer	-
	Peristaltic pump	12V
	Gas flow meter	-
	Measuring cylinder	250ml
	Petri dish	-
	Beaker	100ml
	Plastic basing	5000dm^3

Pneumatic fittings were fixed to the 4M tread hole, and solvent cement was applied to make the systems of the generator and bubbler units fully closed. Fig. 3 illustrates the constructed HHO kit with materials in sub-units.

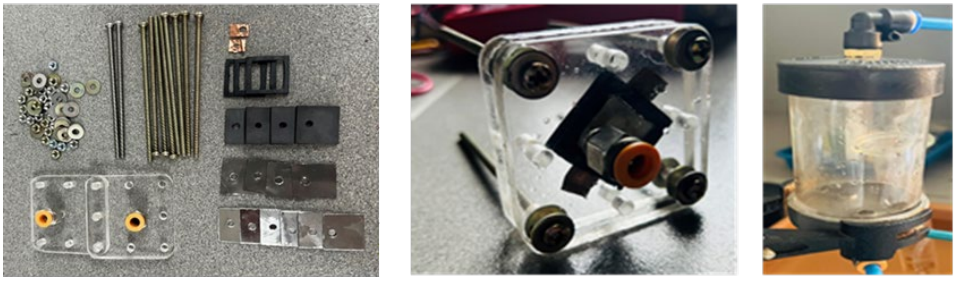

A B C

Fig. 3: Work Completed Electrodes of SS, Graphite and Ti, EPDM Gaskets, Copper Terminals, Acrylic Fixing Plates with SS Nuts, Bolts and Washers (A), Finalized HHO Generator Unit (B), Finalized Bubbler Unit (C)

2.3. Laboratory Testing

The laboratory testing was conducted in two phases. The first phase was conducted to study the behavior of the constructed HHO generator unit. There, the HHO generator was connected to the bench power supply, and its performance was observed under different voltage levels in 1-minute intervals. A peristaltic pump was used to supply the electrolyte at a constant rate of 11 ml/min. Current and voltage readings were taken using a potentiometer with a bench power supply display to measure the voltage addition of the potentiometer. The voltage varied from 0V to 7V. An electrolyte of 0.1M KOH was used, with a 3 mm gap between the electrodes. Generated HHO gas was outed by the outlet line of the bubbler unit; that line was connected to the exhaust line to remove it safely due to the highly flammable gas. The goal was to monitor how the generator behaved under different electrical conditions. Fig. 4 presents phase one of the experimental work.

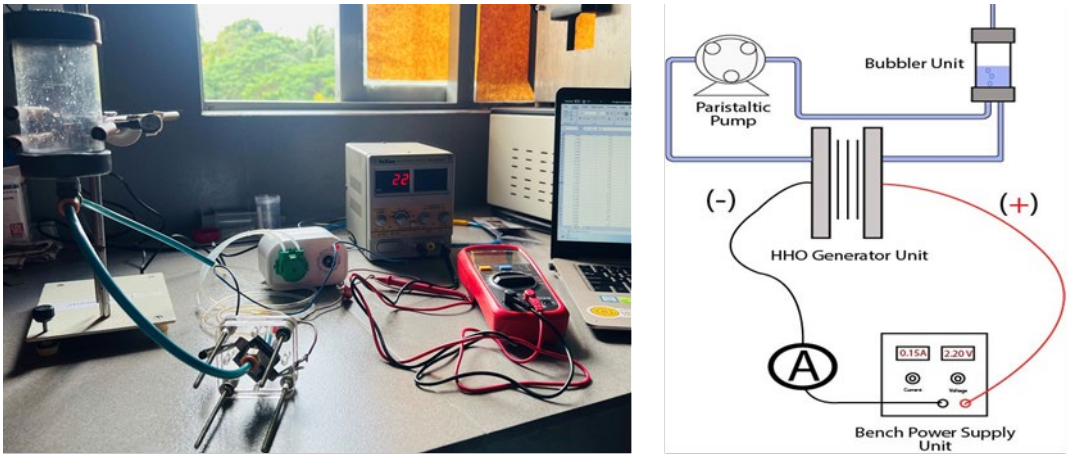

Fig. 4: Apparatus of the whole System (A), Schematic Diagram of the Work (B)

In the second phase, tests were conducted using both KOH and NaOH hydroxides as the electrolytes with 0.08M, 0.1M, and 0.12M molar concentrations because (Chinguwa, Jen, and Akinlabi, 2020) say that the range of KOH and NaOH had resulted ideally. The measuring cylinder apparatus was used to capture and measure the produced gas, and the gas flow meter was used to measure reading further to reduce errors. The electrolyte's flow rate remained 11 ml/min throughout the tests. Various factors, including electrolyte type, electrode material, and voltage (1.4V to 6.4V), were adjusted to determine their effects on the gas production rate and energy consumption during the same time frames to observe optimum configuration. Fig. 5 illustrates phase two of the research work.

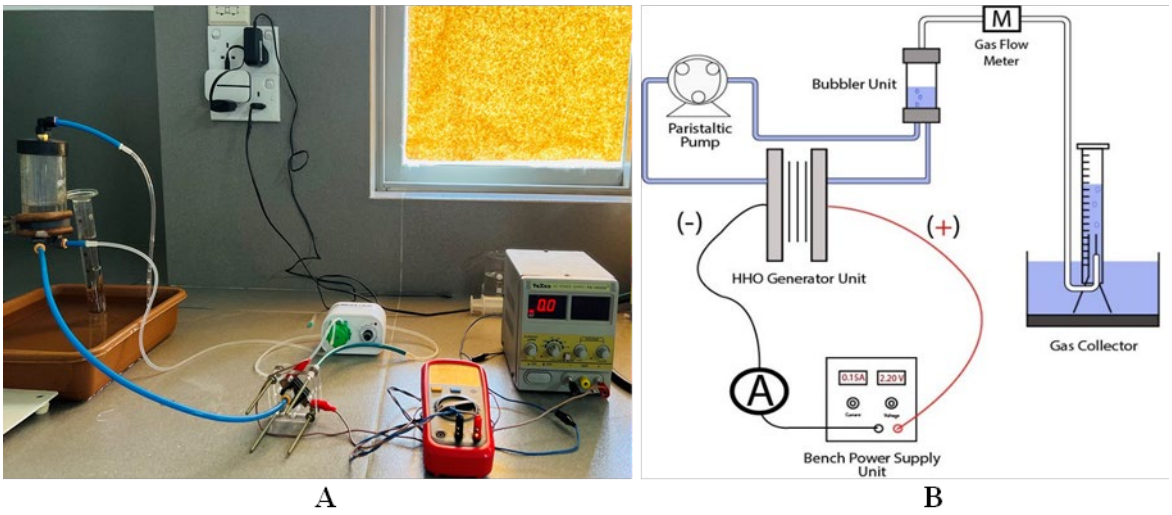

Fig. 5: Apparatus of the Testing (A) Schematic Diagram (B)

2.4. Efficiency Calculation

The efficiency of the HHO generator was determined using Faraday's laws of electrolysis. According to Faraday's law, the amount of gas produced depends on the current passing through the electrolyte. The theoretical volume of gas was calculated using the following Equation 4:

$$V_{theoretical}\,(L) = \frac{I \times t}{n \times F} \times 22.4 \qquad (4)$$

Where I is the current in Amperes (A), t is the time in seconds (s), n is the number of electrons involved, F is Faraday's constant (96485 C/mol), and 22.4 L is the molar volume at Standard conditions.

The actual amount of gas produced was compared to the theoretical value using Equation 5 to calculate how efficiently the generator converted electricity into gas.

$$\text{Faradaic Efficiency \% } (\eta_F) = \frac{\text{V}actual\ (\text{L})}{\text{V}theoretical\ (L)} \times 100 \quad (5)$$

Where ηF represents Faradaic efficiency, $V_{(actual)}$ is the exact volume of gas produced, and $V_{(theoretical)}$ is the expected volume of gas, calculating Equation 4.

Next, Equation 6 calculated the thermodynamic efficiency to determine how much-applied voltage was necessary to split water into hydrogen and oxygen.

$$\text{Thermodynamic Efficiency \% } (\eta_{th}) \frac{1.23V}{\text{V}supply\ (\text{V})} \times 100\% \quad (6)$$

Where 1.23V is the theoretical voltage needed for the water-splitting reaction.

Finally, the overall efficiency of the generator was determined by combining both the Faradaic and thermodynamic efficiencies that represent Equation 7.

$$\eta_t = \eta_{th} \times \eta_F \quad (7)$$

Overall efficiencies of each electrode configuration helped to conclude how well the HHO generator converts electrical energy into gas, considering both the actual gas production and the energy used in the result and discussion section.

3. RESULTS AND DISCUSSIONS

3.1. Gas Production Rate vs Electrolyte Concentration

The gas production rate increased with the higher concentration of both Potassium Hydroxide (KOH) and Sodium Hydroxide (NaOH) across Graphite, SS, and Ti electrode configurations. The graph (Fig. 6) shows production that increased at concentrations above 0.10M due to the higher ion mobility and placing optimum point. The reaction rate is boosted with gas generation. Further, NaOH steadily produced more gas than KOH for all electrode setups. The combination of SS and Graphite also performed flawlessly at a 2.4 ml/min gas production rate at 0.12 M concentration, especially with NaOH. Further, the SS and graphite electrode configuration reached about 1.3-1.4 ml/min at the same concentration of KOH, which was the second-best performance.

Other setups of the SS and Ti combination performed moderately. Combined with Ti, Graphite combined and graphite alone appeared to have the lowest gas production rates for both electrolytes. When graphite acts as an anode, it could accelerate corrosion in nearby metals. Conversely, Ti has lower metal activity than graphite in the Galvanic series. Hence, graphite acts as the cathode, and Ti acts as the anode in this configuration. However, Ti has excellent corrosion resistance due to its ability to form a stable. Overall, SS and Graphite setup with NaOH at 0.1M proved to be the most effective for gas production by graph (Fig. 6).

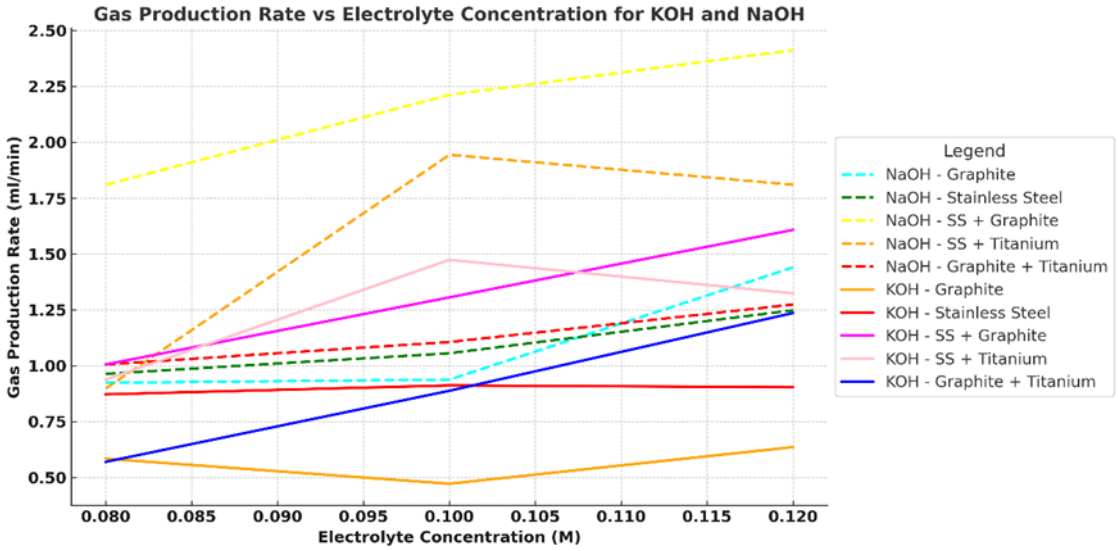

Fig. 6: Gas Production Rate vs Electrolyte Concentration (T = 25 0C, p = 1atm, q = 11ml/min)

3.2. Gas Production Rate vs Voltage

The results in Fig. 7 show that the effect of the gas production rate increases proportionally with the voltage of all electrode configurations. The SS and Graphite combination demonstrated the highest gas production rate of approximately 0.234 ml/min at 2.6 V. This setup consistently outperforms others, indicating high efficiency in generating gas at higher voltages. Graphite alone and graphite combined with Ti show much lower gas production rates, with minimal gas output at lower voltages and slower increases as voltage rises. SS alone shows moderate performance but is significantly outperformed by the combination of SS Steel and Graphite. This trend suggests that pairing different electrode materials, particularly SS with Graphite, greatly enhances gas production efficiency as voltage increases.

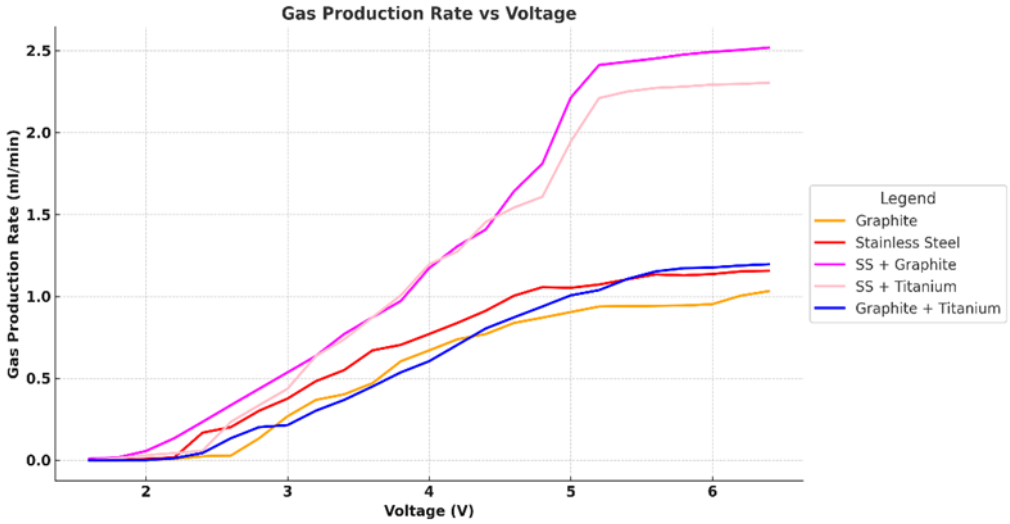

Fig. 7: Gas Production Rate vs Voltage (C = 0.1M, T = 25 0C, p = 1atm, q = 11ml/min)

3.3. Gas Production Rate vs Current

The gas production rate increases with the current across different electrode configurations of Graphite, SS, and Ti. Higher current levels require more energy to drive the electrochemical reactions responsible for more gas generation. Including all setups, the combination of SS and Graphite steadily produced the most HHO

gas of approximately 0.234 ml/min at a current of 0.06 A, which is shown in Fig. 8. SS alone performed moderately, with its gas production rate steadily rising to around 0.168 ml/min at similar current levels. Other setups, such as Graphite alone and Graphite combined with Ti, showed significantly lower gas production rates. These configurations generated minimal gas at lower current levels and exhibited slower increases in production as the current rose. The combination of SS and Ti also performed moderately, with a maximum gas production rate of around 0.058 ml/min.

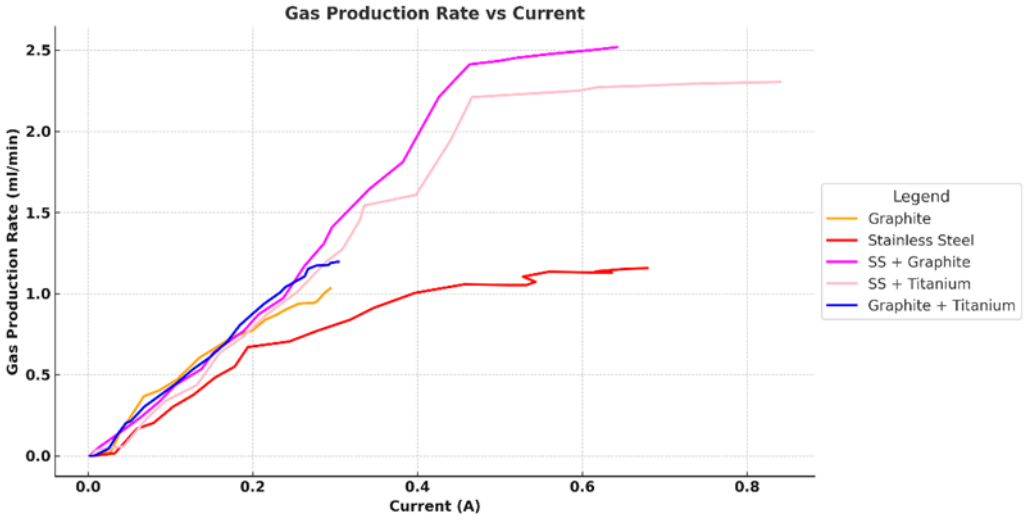

Fig. 8: Gas Production Rate vs Current (C = 0.1M, T = 25 0C, p = 1atm, q = 11ml/min)

3.4. Current vs Voltage

The current increased with rising voltage for all electrode configurations due to Ohm's law. The combination of SS and Ti shows the most significant current enhancement, especially at higher voltages above 2.6 V with 0.09 A. This combination emphasizes higher current flow, potentially due to improved conductivity between the two materials. Graphite alone shows the least current, remaining relatively low even as voltage increases. Other SS and Graphite combinations show steady increases in current, but not higher than the SS and Ti combination. This pattern highlights that the choice of electrode material affects the current flow, with the material Ti offering better conductivity when paired with others. According to Fig. 9, SS and Graphite yield the best gas production performance compared with SS and Ti because SS and Graphite configuration performed more similarly leaner distribution with more sooner to one of R2 value considering operational priorities. Hence, SS and TI performed as second-best configurations.

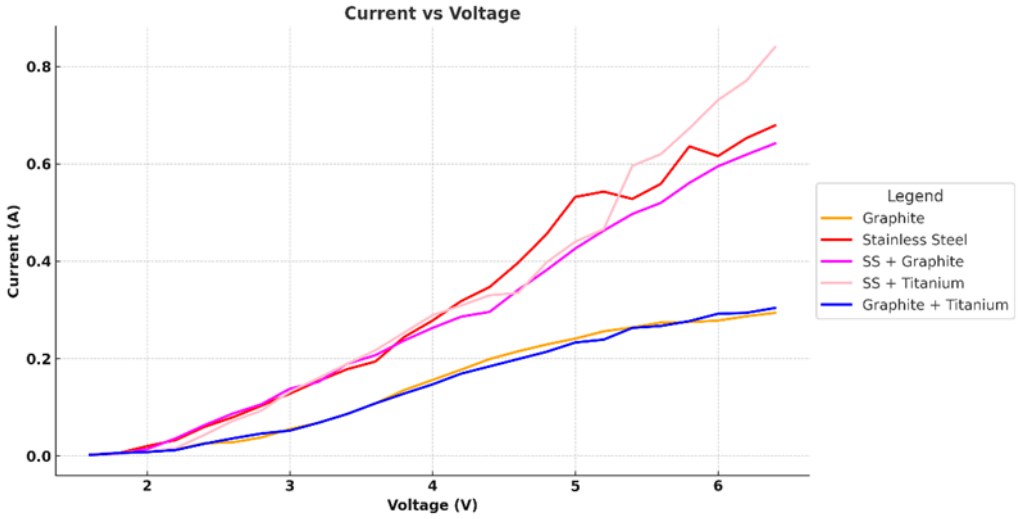

Fig. 9: Current vs Voltage (C = 0.1M, T = 25 0C, p = 1atm, q = 11ml/min)

3.5. Efficiency Comparison of Electrode Materials

The bar chart (Fig. 10) compares different electrode materials based on overall efficiency calculated from Faradaic efficiency (ηF) and thermodynamic efficiency (ηth). The data shows that SS and Ti achieved the highest efficiency, 24.6%, and the second highest was SS and Graphite, 23.1%. The combination of Graphite and Ti had a moderate efficiency of 19.8%. Graphite alone reached 20.1%, and SS alone had the lowest efficiency, at 12.6%.

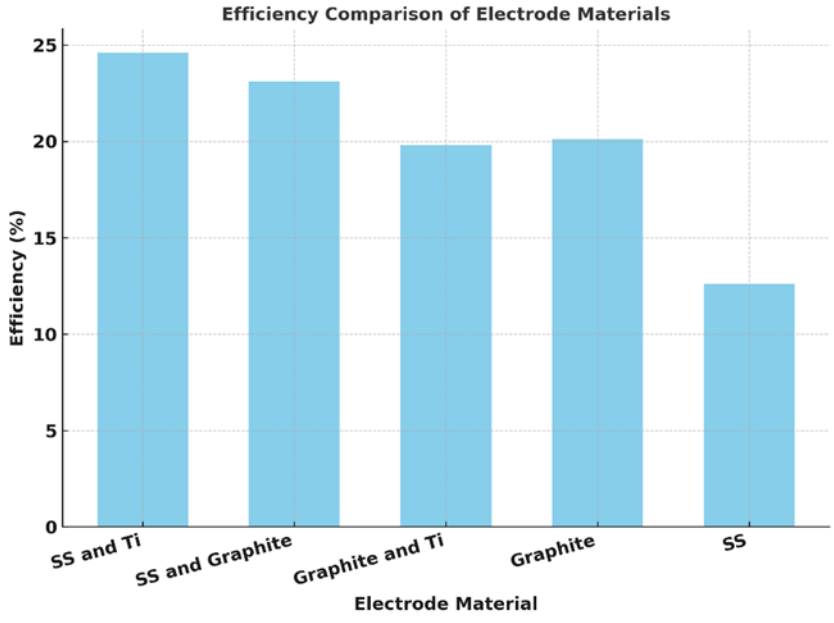

Fig. 10: Efficiency Comparison of Electrode Materials (C = 0.1M, T = 25 0C, p = 1atm, q = 11ml/min)

Furthermore, efficiency reduction was significantly attributed to high-potential scenarios like heat generation and electrode surface oxidation. Surface reduction degrades materials and reduces performance. Electrodes can oxidize on their surface according to the electrochemical dynamics. In this environment, NaOH acts as a strong electrolyte, dissociating into Na^+ and OH^- ions and facilitating electrolysis. Hence, due to their intrinsic material properties and electrochemical behavior, graphite electrodes oxidize more readily than SS and Ti when used as an anode in an alkaline HHO generator. Fig 11 illustrates the oxidation results of graphite as an anode

application and Ti electrode as a cathode at 20 to 30 minutes of operation. Graphite comprises carbon atoms arranged in a layered structure with weak van der Waals forces between the layers. This structure provides high electrical conductivity but also exposes edge sites and defects, which are highly reactive. In an alkaline NaOH solution, these reactive sites are susceptible to attack by OH^- ions, forming CO_2 or carbonate ions, which degrade the graphite structure.

Fig. 11: Electrolyte Color Change by Metal Oxidation (A), Appearance of Graphite and Ti electrode surfaces after oxidation (B)

In contrast, SS and Ti form stable, protective oxide layers of Cr_2O_3 for SS and TiO_2 for Ti on their surfaces when exposed to oxidative environments. These passive layers significantly reduce the rate of further oxidation and protect the underlying material from degradation. Graphite, lacking such a protective mechanism, remains exposed to continuous attack by the electrolyte, leading to higher oxidation rates. Moreover, graphite's relatively lower overpotential for anodic reactions facilitates oxidation at a lower applied voltage, making it less durable than SS and Ti under similar conditions. It makes graphite less favorable for long-term use as an anode in highly oxidative environments.

4. CONCLUSIONS

The study successfully optimized the performance of a dry-type alkaline HHO electrolyzer, emphasizing the effects of electrode materials, electrolyte concentration, and applied voltage on gas production efficiency. Among various configurations, SS paired with Ti and a 0.12M NaOH solution achieved the highest gas production efficiency at 24.6%. SS paired with graphite scored 23.1%, getting the second-highest result. Further, the optimum voltage range is 4.5V to 5.2V for SS with graphite and 4.2V to 5.2V for SS with Ti configurations. The results demonstrate that increasing the voltage enhances gas output and leads to electrode degradation due to surface oxidation, which limits long-term efficiency.

Furthermore, with 0.12M, NaOH was a more suitable electrolyte than KOH, promoting higher gas production rates. This research provides a clear path for enhancing HHO gas production while minimizing energy consumption and preventing electrode deterioration. The findings support optimized HHO systems integrating into two-wheeler vehicle four-stroke ICEs to improve fuel efficiency and reduce GHG emissions. The next phase of this research will involve integrating the system with 100cc gasoline internal combustion engines (ICE) in two-wheeled vehicles. This approach could support broader adoption and contribute to further reductions in emissions. Hence, it can extend its positive application to three-wheel and four-wheel vehicles in future improvements.

Author Contributions: Conceptualization and methodology, M.B.D.K. Siriwardena and A.R. Nihmiya; writing—original draft preparation, M.B.D.K. Siriwardena; writing—review and editing, A.R. Nihmiya, Udara S.P.R. Arachchige and Gamunu S. Arachchige; supervision, A.R. Nihmiya, Udara S.P.R. Arachchige and Gamunu S. Arachchige. All authors have read and agreed to the published version of the manuscript.

Funding: This research was funded by Norwegian Partnership Programme for Global Academic Cooperation (NORPART) project, grant number NORPART-2021/10175.

Conflicts of Interest: The authors declare that they have no conflicts of interest..

5. REFERENCES

1. Arjun, T.B. et al. (2019a) 'A review on analysis of HHO gas in IC engines', Materials Today: Proceedings, 11, pp. 1117–1129.
2. Arjun, T.B. et al. (2019b) 'A review on analysis of HHO gas in IC engines', Materials Today: Proceedings, 11, pp. 1117–1129.
3. Bard, A.J. and Faulkner, L.R. (2001) Electrochemical Methods: Fundamentals and Applications. 2nd edn. New York: Wiley. ISBN: 978-0471043720.
4. Bockris, J.O., Gamboa-Aldeco, M. and Reddy, A.K.N. (2002) Modern Electrochemistry 2A: Fundamentals of Electronics. 2nd edn. New York: Kluwer Academic Publishers. ISBN: 978-0306461675.
5. Chinguwa, S., Jen, T.C. and Akinlabi, E.T. (2020) 'Conceptualization of the optimal design of a hydroxyl booster dry cell for enhancing the efficiency of internal combustion engines,' Procedia CIRP, 88, pp. 819–823. https://doi.org/10.1016/j.procir.2020.03.118.
6. Wang, F. (2021) 'Arduino-based control systems in small-scale hydrogen production,' International Journal of Hydrogen Energy, 46(5), pp. 3270–3281. https://doi.org/10.1016/j.ijhydene.2020.10.202.
7. Fuller, T.F. and Harb, J.N. (2018) Electrochemical Engineering. Hoboken, NJ: John Wiley & Sons. ISBN: 978-1119004127.
8. Huang, J. and Wang, Y. (2020) 'Efficient renewable-to-hydrogen conversion via decoupled electrochemical water splitting,' Cell Reports Physical Science, 1(1), p. 100138. https://doi.org/10.1016/j.xcrp.2020.100138.
9. Jones, L.E. (2014) Renewable Energy Integration. London: Academic Press. ISBN: 978-0124079106.
10. Khandal, S.V. et al. (2022) 'Influences of hydrogen addition from different dual-fuel modes on engine behaviors,' Energy Science & Engineering, 10(3), pp. 881–891. https://doi.org/10.1002/ese3.1065.
11. Yurukcu, M. et al. (2021) 'Advanced materials for next-generation fuel cells', in Advanced Nanomaterials for Electrochemical-Based Energy Conversion and Storage. Amsterdam: Elsevier, pp. 213–266. https://doi.org/10.1016/B978-0-12-824379-4.00003-3.
12. Newman, J. and Thomas-Alyea, K.E. (2012) Electrochemical Systems. 3rd edn. Hoboken, NJ: John Wiley & Sons. ISBN: 978-0471750444.
13. Rimkus, A., Mejeras, G. and Matijošius, J. (2023) 'The influence of hydrogen and oxygen (HHO) gas on engine characteristics under the effect of the lean mixtures of gasoline and bioethanol,' International Journal of Hydrogen Energy, 48(99), pp. 39612–39624. https://doi.org/10.1016/j.ijhydene.2023.07.167.
14. Rinawati, D.I. et al. (2022) 'Life-cycle assessment of hydrogen utilization in power generation: A systematic review of technological and methodological choices,' Frontiers in Sustainability, 3, p. 920876. https://doi.org/10.3389/frsus.2022.920876.
15. Rusdianasari, Yohandri, B. and Dewi, T. (2019) 'HHO gas generation in hydrogen generator using electrolysis,' IOP Conference Series: Earth and Environmental Science, 258, p. 012002. https://doi.org/10.1088/1755-1315/258/1/012002.
16. Sivakumar, B. et al. (2021) 'Generation of brown gas from a dry cell HHO generator using chemical decomposition reaction,' IOP Conference Series: Materials Science and Engineering, 1130(1), p. 012002. https://doi.org/10.1088/1757-899X/1130/1/012002.
17. Petrovic, S. and Hossain, E. (2020) 'Development of a novel technological readiness assessment tool for fuel cell technology,' IEEE Access, 8, pp. 123456–123470. https://doi.org/10.1109/ACCESS.2020.3009193.
18. Wilberforce, T. and Olabi, A.G. (2020) 'Design of experiment (DOE) analysis of 5-cell stack fuel cell using three bipolar plate geometry designs', Sustainability, 12(11), p. 4488. https://doi.org/10.3390/su12114488.
19. Zohuri, B. (2018) Hybrid Energy Systems: Driving Reliable Renewable Sources of Energy Storage. 1st edn. Cham: Springer. ISBN: 978-3319705515.